EUROPEAN SYNCHROTRON RADIATION FACILITY

INSTALLATION EUROPEENNE DE RAYONNEMENT SYNCHROTRON

ESRF

Experiment Report Form

The double page inside this form is to be filled in by all users or groups of users who have had access to beam time for measurements at the ESRF.

Once completed, the report should be submitted electronically to the User Office via the User Portal:

https://wwws.esrf.fr/misapps/SMISWebClient/protected/welcome.do

Reports supporting requests for additional beam time

Reports can be submitted independently of new proposals – it is necessary simply to indicate the number of the report(s) supporting a new proposal on the proposal form.

The Review Committees reserve the right to reject new proposals from groups who have not reported on the use of beam time allocated previously.

Reports on experiments relating to long term projects

Proposers awarded beam time for a long term project are required to submit an interim report at the end of each year, irrespective of the number of shifts of beam time they have used.

Published papers

All users must give proper credit to ESRF staff members and proper mention to ESRF facilities which were essential for the results described in any ensuing publication. Further, they are obliged to send to the Joint ESRF/ ILL library the complete reference and the abstract of all papers appearing in print, and resulting from the use of the ESRF.

Should you wish to make more general comments on the experiment, please note them on the User Evaluation Form, and send both the Report and the Evaluation Form to the User Office.

Deadlines for submission of Experimental Reports

- 1st March for experiments carried out up until June of the previous year;
- 1st September for experiments carried out up until January of the same year.

Instructions for preparing your Report

- fill in a separate form for each project or series of measurements.
- type your report, in English.
- include the reference number of the proposal to which the report refers.
- make sure that the text, tables and figures fit into the space available.
- if your work is published or is in press, you may prefer to paste in the abstract, and add full reference details. If the abstract is in a language other than English, please include an English translation.

	Experiment title: μ-XRF and μ-XANES analysis for disclosing the role of metallic silver on the darkening process of yellow-orange arsenic-sulfide pigments in a Cimabue's painting (13th C.)	**Experiment number**: HG-117
Beamline: ID21	**Date of experiment**: from: 29/11/2017 to: 04/12/2017	**Date of report**: 02/03/2020
Shifts: 12	**Local contact(s)**: Marine Cotte	*Received at ESRF:*

Names and affiliations of applicants (* indicates experimentalists):

* Letizia Monico, Department of Chemistry, Biology and Biotechnology, University of Perugia, Italy

* Emilio Catelli, Department of Chemistry, Bologna University, Italy

* Gert Nuyts, Department of Chemistry, Antwerp University, Belgium

	Experiment title: μ-XRF and μ-XANES analysis for disclosing the role of metallic silver on the darkening process of yellow-orange arsenic-sulfide pigments in a Cimabue's painting (13th C.)	**Experiment number**: HG-117
Beamline: ID16b	**Date of experiment**: from: 14/02/2018 to: 18/02/2018	**Date of report**: 02/03/2020
Shifts: 12	**Local contact(s)**: Vanessa isabel Tardillo suarez	*Received at ESRF:*

Names and affiliations of applicants (* indicates experimentalists):

* Gert Nuyts, Department of Chemistry, Antwerp University, Belgium

* Emilio Catelli, Department of Chemistry, Bologna University, Italy

* Andrea Marchetti, Department of Chemistry, Antwerp University, Belgium

1. INTRODUCTION

During the two experiments we have investigated the effect of metallic silver (Ag^0) on the darkening of the yellow-orange pigments orpiment (As_2S_3) and realgar (As_4S_4). The phenomenon has been observed in micro-samples taken from "*Madonna Enthroned with the Child and Two Angels*" attributed to Cimabue (1240–1302) (Figure 1). Based on previous studies, we have proposed that both/one of the following pathways is the cause of darkening:

1) a photochemical reaction between As_2S_3/As_4S_4, oxygen and moisture entrapped in the surrounding organic binder and/or arising from the environment, which may lead to the formation of As_2O_3 (arsenolite)/$H_3As_2O_3$ and SO_2/SO_4^{-2}/thioarsenite species; acidic environmental conditions might then promote the solubilization and oxidation of As_2O_3/arsenites (As^{+3}) to arsenates (As^{+5}) [1-6]. The parallel oxidation of Ag^0 to Ag^+ might occur locally, followed by the precipitation of AgS-based materials and of Ag_3AsO_4 and/or Ag_3AsO_3.

2) a photo-dissolution of Ag^+ cations in the As_2S_3 paint matrix, involving the direct photo-oxidation of Ag^0 to Ag^+ as a first step of reaction, leading to *in situ* formation of Ag_2S and subsequent production of various Ag-As-S ternary compounds as final products [7-8].

With the aim to gaining insights into which between the two above mechanisms actually is the most probable one, we have performed μ-XRF and μ-XANES analysis at S K-/Ag L_3-edges (ID21) and at As K-edge (ID16b) on a series of artificially aged model samples and on historical paint-samples (Figure 1).

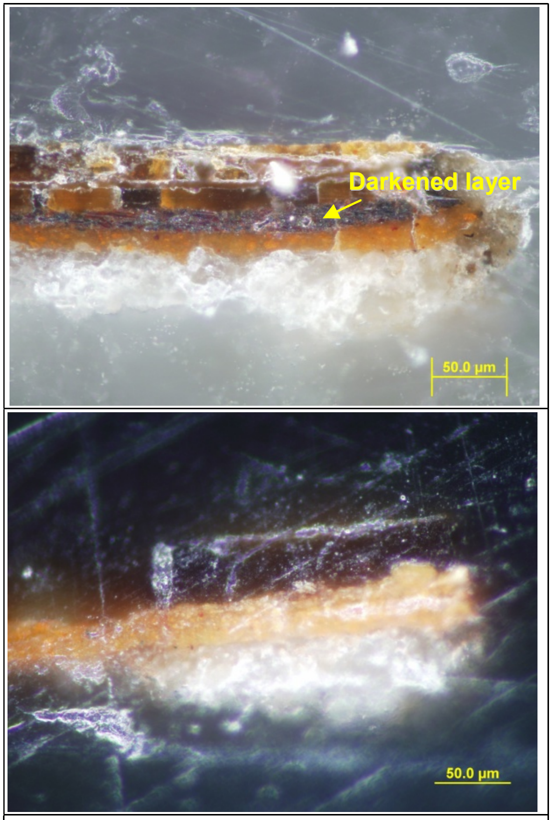

Figure 1. Photomicrograph of a selection of the analyzed cross-sections obtained from *"Madonna Enthroned with the Child and Two Angels"* attributed to Cimabue (Bologna, Italy). (top) fragment taken from a darkened area; (bottom) sample obtained from a not-darkened region.

2. EXPERIMENTAL

The list of samples that we have analyzed at beamlines ID21 and ID16b is reported below:

a) Arsenic sulfide-based model samples (ca. 30 in total) mixed either with egg or linseed oil and in presence or absence of metallic silver before and after exposure to different aging conditions (of light and relative humidity);

b) Original paint micro-fragments (4 in total) obtained from selected (un)darkened regions of the painting "*Madonna Enthroned with the Child and Two Angels*".

c) set of S-, Ag- and As-reference powders (ca. 15 in total).

All paint samples (models and historical ones) have been investigated in the form of embedded resin cross-sections both at ID21 and ID16b beamlines. Only at ID21, additional measurements have been carried out at the surface of not-embedded resin fragments of the model samples.

Each reference powder has been analyzed as a thin film (thickness< 50 μm) fixed on sulfur-free tape.

• *ID21-experimental set-up*. μ-XRF and μ-XANES measurements at S K-edge (2.4720 keV) and Ag L_3-edge (3.3511 keV) were performed at the scanning X-ray microscope (SXM) end-station by means of a fixed exit double-crystal Si(111) monochromator.

The incident beam was focused with Kirkpatrick-Baez (KB) mirrors down to a diameter of *ca.* 0.6×0.4 μm² (h×v). The energy calibration was performed at the S K-edge and Ag L_3-edge by setting the position of the peak maximum of the first order derivative spectrum of gypusm and of a metallic silver foil at 2.4829 keV and 3.3547 keV, respectively.

XRF signals were collected in the horizontal plane and at 69° with respect to the incident beam direction by means of a single energy-dispersive silicon drift detector (Xflash 5100, Bruker).

Single point μ-XANES spectra were acquired in XRF mode by scanning the primary energy around the S K-edge (2.46-2.53 keV; energy step: 0.17 eV) and Ag L_3-edge (3.34-3.42 keV; energy step: 0.25 eV).

μ-XRF mapping experiments were performed using a monochromatic primary beam of fixed energy around the S K-edge. Maps of the same region of interest were collected by employing 100 ms/pixel at the three following energies: (i) 2.4718 keV and (ii) 2.4827 keV to favor the excitation of the S^{-II}- and S^{VI}-species, respectively and (iii) 3.4 keV to obtain the XRF intensity of all S- and Ag-species.

• *ID16b-experimental set-up*. μ-XRF and μ-XANES investigations at As K-edge (11.8667 keV) were performed by means of a fixed exit double-crystal Si(111) monochromator. KB mirrors were employed for focussing the incident beam down to a diameter of *ca.* 0.1×0.1 μm² (h×v). XRF signals were collected by means of a Si drift-diode array detector.

Single point μ-XANES spectra were recorded in XRF mode by scanning the primary energy across the As K-edge (11.78-12.16 keV; energy step: 1 eV). μ-XRF maps of the same region of interest were collected using 100 ms/pixel at the three following energies: (i) 11.8715 keV and (ii) 11.8786 keV to favor the excitation of the As^{III}-sulfides and As_2O_3 /As^{V}-species, respectively and (iii) 12.0 keV to obtain the XRF intensity of all As-species.

Fitting of the μ-XRF spectra and elaboration of the elemental maps at the different energies recorded at both beamlines were performed using the PyMca sofware, while further processing of the different elemental distribution maps was done by means of the XRDUA sofware package. [9] ATHENA [10] was employed to perform the normalization of the XANES spectra.

3. RESULTS

3.1. Artificially aged arsenic sulfides-based model paints.

As an example the SR μ-XRF and μ-XANES results obtained from a UVA-Visible light exposed egg paint mock-up, prepared by mixing orpiment (As_2S_3) and metallic silver (Ag^0) (in a 3:1 weight ratio), are shown in Figure 2.

Before aging (results not reported), S-, Ag- and As-speciation investigations reveal that only As_2S_3 along with metallic silver particles are present in the sample.

As a result of the light exposure, a strong darkening is visible at the paint surface (Figure 2A-B). As- and S-speciation maps (Figure 2C,E) along with μ-XANES investigations (Figure 2D,F,G) reveal that the dark layer visible in the uppermost side of the paint is composed of As_2O_3 (Figure 2D: pts 01_{As}-04_{As}), Ag_2S (Figure 2G: pts 01_{Ag}-02_{Ag}), As_2S_3 and minor abundances of sulfates (Figure 2F: pts 01_S-03_S). In the bulk-yellow paint underneath, As_2S_3 is the dominant component (Figure 2D,F: pts 05_{As}-11_{As}; pts 04_S-05_S), along with localized spots of Ag_2S, Ag^0 (Figure 2G: pt 03_{Ag}, 04_{Ag}), and sulfates (Figure 2F: pt 03_S).

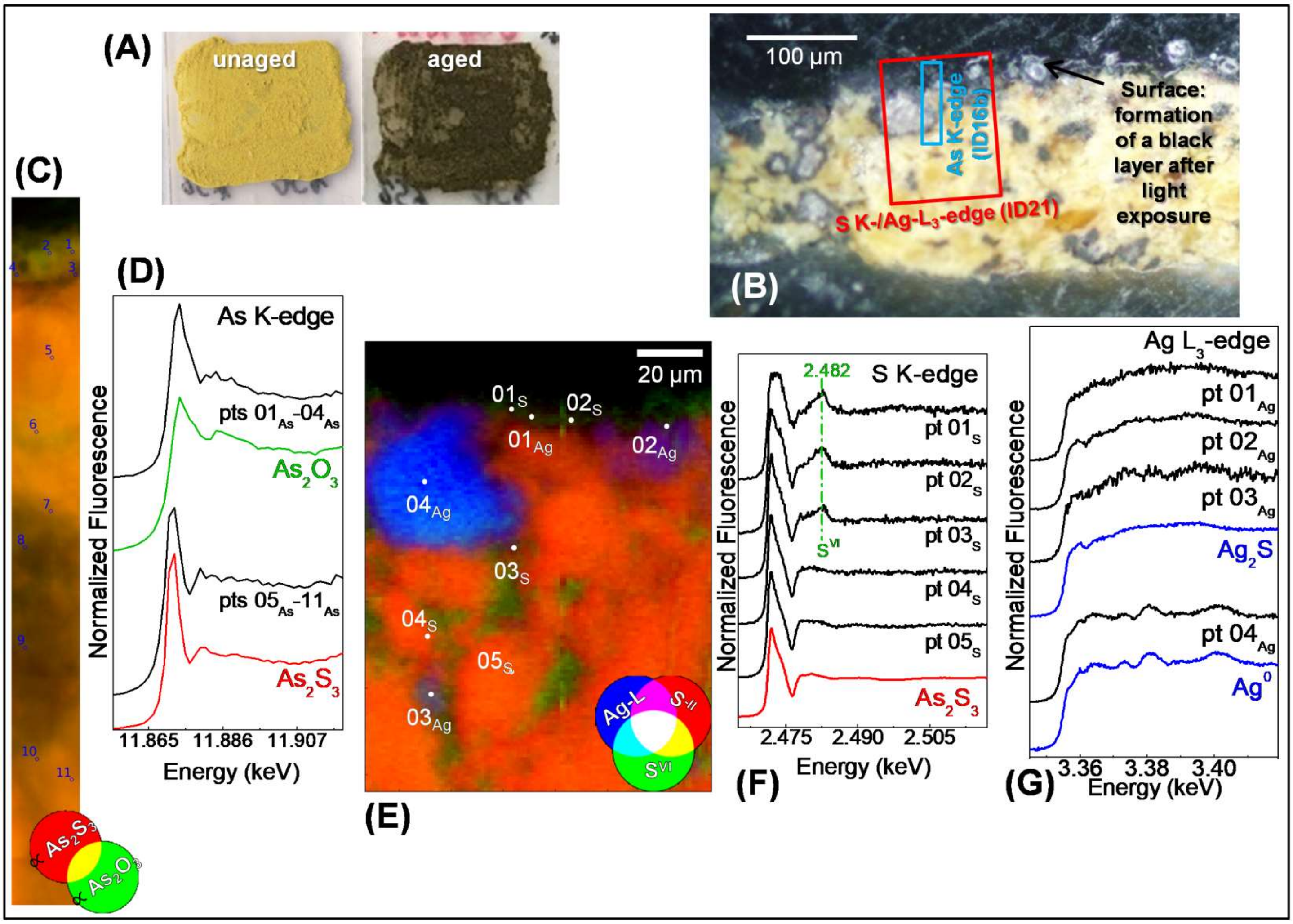

Figure 3. (A) Photographs of egg paint models composed of a mixture of orpiment and metallic silver (left) before and (right) after UVA-Visible light exposure. (B) Photomicrograph of a cross-section obtained from a fragment of the aged paint shown in (A). (C) Composite RG As-speciation maps (step size: 0.1×0.1 μm^2, exp. time: 100 ms/pixel) and (D) selection of the corresponding As K-edge μ-XANES spectra compared to those of reference compounds (data recorded at ID16b). (D) Composite RGB SR μ-XRF maps of S^{-II}/S^{VI}/Ag (step size:: 1×1 μm^2, exp. time: 100 ms/pixel) and selection of the corresponding (F) S K-edge and (G) Ag L3-edge μ-XANES spectra compared to the profiles of a set of reference compounds (data collected at ID21).

Comparable results were obtained from the equivalent egg paint prepared with the pigment realgar and aged using similar conditions. In the absence of metallic silver and after exposure to light, the "pure" orpiment and realgar egg paints revealed the formation of localized spots of sulfates and As_2O_3 at the surface (results not shown).

Regardless to the presence of Ag^0, we have also found that the tendency of arsenic sulfide-based pigments towards degradation increases, when linseed oil is used as binding medium (data not reported). At this regard, the measurements have revealed that a superficial degradation layer composed of As_2O_3, As^V-species and sulfates, is already present in the paints before artificial aging.

3.2 Original paint micro-samples taken from "Madonna Enthroned with the Child".

Figure 3 shows the S-, Ag- and As-speciation results recorded from an original paint micro-sample taken from a darkened region of the painting "*Madonna Enthroned with the Child and Two Angels"* (as an example, only the results of one of the analyzed cross-sections are reported).
S-speciation measurements performed in the darkened Ag-rich layer (Figure 3A-C) reveal that variable amounts of sulfides (S^{-II}) and sulfates (S^{VI}) are present. The Ag L_3-edge XANES spectra recorded from selected spots of the same layer, strongly resemble that of Ag_2S (Figure 3D). In addition, As-speciation investigations (Figure 3E,F) permitted to identify both As^{III}- and As^{V}-compounds, the latter likely arising from a degradation process of the original arsenic-sulfide based pigment.

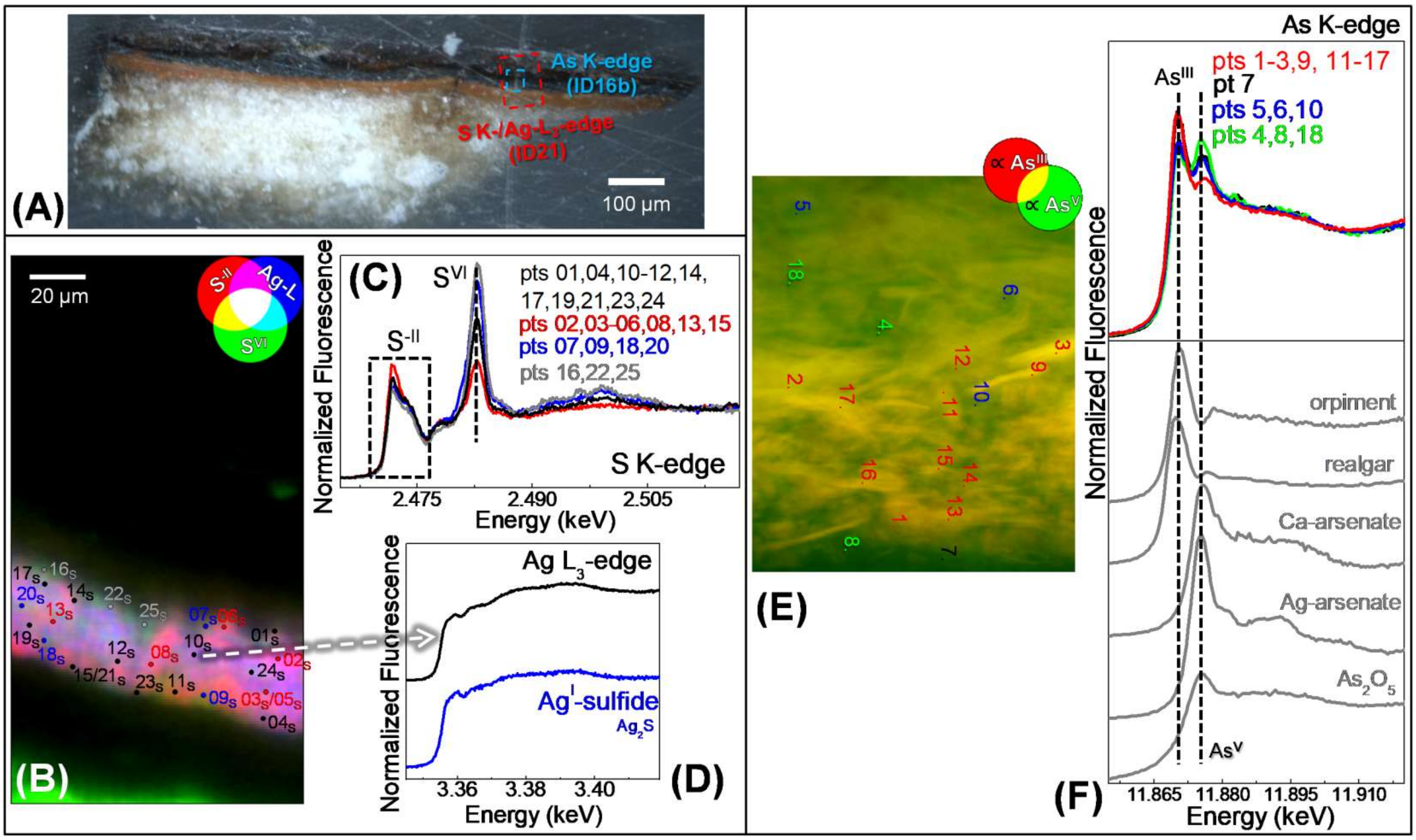

Figure 3. (A) Photomicrograph of a cross-section of a fragment taken from a darkened region of the painting "*Madonna Enthroned with the Child and Two Angels"* (Bologna, Italy). (B) Composite RGB SR µ-XRF maps of $S^{-II}/S^{VI}/Ag$ [step size (v×h): 0.5×0.7 μm^2, exp. time: 100 ms/pixel] and selection of the corresponding (C) S K-edge and (D) Ag L_3-edge µ-XANES spectra compared to the profiles of reference compounds (data collected at ID21). (E) Composite RG As-speciation maps (step size: 0.1×0.1 μm^2, exp. time: 100 ms/pixel) and (F) selection of the corresponding As K-edge µ-XANES spectra compared to those of a set of reference compounds (data recorded at ID16b).

Overall the results obtained from the study of artificially aged model paints and historical paint-samples reveal that Ag^0 plays a key role in the darkening process of arsenic sulfide-based paints, giving rise to Ag_2S as secondary compound. At the same time, the formation of additional degradation products, including sulfates, As_2O_3 and/or As^V-compounds, may take place.

The data acquired during the experiments also permitted to reveal that the tendency towards degradation of arsenic-sulfide pigments strongly depends on the nature of the binding medium, being more pronounced in the presence of linseed oil instead of egg.

The results obtained from this experiment are expected to be published soon.

REFERENCES:

[1] M. Vermeulen, et al., *Journal of Analytical Atomic Spectrometry* (2016), **31**, 1913-1921; [2] K. Keune, et al., *Journal of Analytical Atomic Spectrometry* (2015), **30**, 813-827; [3] K. Keune, et al., *Heritage Science* (2016), **4.1**, 10; [4] M. F. Lengke, et al., *The Canadian Mineralogist* (2009), **47**, 593-613; [5] L. Xiandong, et al., *Chemical Geology* (2015), **411**, 192-199; [6] R. T., Wilkin, et al., *Geochemical Transactions* (2003), **4**, 1-7; [7] D. Tsiulyanu, *Journal of Non-Crystalline Solids* (2010), **356**, 147–152; [8] M. Mitkova, M. N. Kozicki, Fourfold Coordinated Silver-containing Chalcogenide Glasses – Basic Science and Applications in Optical Programmable Metallization Cell (PMC), in *Technologies in Optoelectronic Amorphous Materials and Devices*, G. Lucovsky and M. Popescu Editors, INOE Publ. House, 2004; [9] W. De Nolf et al., *Journal of applied crystallography* (2014), **47**, 1107-1117; [10] B. Ravel, M. J. Newville, *Journal of Synchrotron Radiation* (2005), **12**, 537–541.